

Momentum dependence of K^- -nuclear potentials

L. Dang,^{1,*} L. Li,^{1,†} X. H. Zhong,^{2,‡} and P. Z. Ning^{1,§}

¹*Department of Physics, Nankai University, Tianjin 300071, People's Republic of China*

²*Institute of High Energy Physics, Chinese Academy of Sciences, Beijing 100039, People's Republic of China*

(Received 1 February 2007; revised manuscript received 28 March 2007; published 21 June 2007)

The momentum dependent K^- -nucleus optical potentials are obtained based on the relativistic mean-field theory. By considering the quarks coordinates of K^- meson, we introduced a momentum-dependent “form factor” to modify the coupling vertexes. The parameters in the form factors are determined by fitting the experimental K^- -nucleus scattering data. It is found that the real part of the optical potentials decrease with increasing K^- momenta, however the imaginary potentials increase at first with increasing momenta up to $P_k = 450 \sim 550$ MeV and then decrease. By comparing the calculated K^- mean free paths with those from K^-n/K^-p scattering data, we suggested that the real potential depth is $V_0 \sim 80$ MeV, and the imaginary potential parameter is $W_0 \sim 65$ MeV.

DOI: [10.1103/PhysRevC.75.068201](https://doi.org/10.1103/PhysRevC.75.068201)

PACS number(s): 21.65.+f, 13.75.Jz, 21.30.Fe, 24.10.Ht

Recently kaon nuclear physics has been a hot topic of nuclear physics, and kaon-nucleus interaction is a key point to many studies on kaon. The information of K^- -nucleus interaction were obtained from K^- -atomic and K^-N scattering data. Since the kaon is only sensitive to the surface structure of nuclei in K^- -atomic, predictions on K^- -nucleus interactions are very different for different models (a very strong attractive real potential, 150 \sim 200 MeV, from the density dependent optical potential (DD) model [1,2]; and a much shallower one \sim 50 MeV from the chiral model [3]). On the other hand, Sibirtsev *et al.* predicted the kaon-nucleus interaction has “momentum dependence” from K^-N scattering data [4]. They have obtained a momentum dependent potential in a dispersion approach at normal nuclear density, the potential depth is about 140 ± 20 MeV at zero momentum, and decreases rapidly for higher momenta. In our previous work [5], we also found that the kaon nucleus optical potential has strong momentum dependence by fitting the only experimental data on the K^-C , K^-Ca scattering at $P_k = 800$ MeV/c [6]. We indicated that the depth of real potential at the inner nuclei is (45 ± 5) MeV at $P_k = 800$ MeV/c, which is much shallower than that at zero momentum in the relativistic-mean field (RMF). We shall here be concerned with discussing the momentum dependence of K^- -nucleus interaction within the framework of the RMF.

In the usual RMF model, one cannot obtain the correct momentum dependence of the K^- -nucleus interaction, and would have to take the internal structure of kaon into account to introduce a momentum-dependent “form factor” [7]. When RMF is extended to study KN interaction at the quark level, the same approximation as made in the quark-meson coupling (QMC) model [8,9] should be introduced: σ - and ω -mesons are exchanged only between the u , d quarks or their antiquarks in the K meson, contributions from the s quark are ignored. In the following, we shall take the kaon as a two quarks system

to introduce an exponential “form factor”, $\exp(-P_k^2/4\kappa^2)$, which will modify the couplings vertexes. In fact, a similar exponential “form factor” has been widely adopted to improve various calculations [10–12].

In the RMF, the KN interactions are described by exchanging scalar meson σ and vector meson ω [13]. At the quark level, σ - and ω -mesons are exchanged between the u , d quarks or their antiquarks. As in Fig. 1, the scalar and vector couplings are

$$\mathcal{L}_\sigma = g_{\sigma K} m_K \bar{K} \sigma K, \quad (1)$$

$$\mathcal{L}_\omega = i g_{\omega K} \bar{K} \omega^\mu \partial_\mu K + \text{H.c.} \quad (2)$$

Replacing the scalar meson σ and vector meson ω with their plane wave form to get

$$\mathcal{L}_\sigma = g_{\sigma K} m_K \bar{K} (a_\sigma e^{-i\mathbf{q}\cdot\mathbf{r}_2}) K, \quad (3)$$

$$\mathcal{L}_\omega = i g_{\omega K} \bar{K} (a_\omega e^{-i\mathbf{q}\cdot\mathbf{r}_2} \varepsilon^\mu) \partial_\mu K + \text{H.c.}, \quad (4)$$

where \mathbf{r}_2 represents the coordinates of u/d quarks, with respect to the center of mass coordinates \mathbf{R} and the relative coordinates \mathbf{r} in the quark model. And we assume $\mathbf{q} = c\mathbf{P}_k$ approximately as the transferred momentum being proportional to K^- incidence momentum. Thus,

$$e^{-i\mathbf{q}\cdot\mathbf{r}_2} = e^{-ic\mathbf{P}_K \cdot \mathbf{R}} e^{\frac{i\mu}{m_2} c\mathbf{P}_K \cdot \mathbf{r}}. \quad (5)$$

On the harmonic-oscillator basis, if the relative coordinates \mathbf{r} is rewritten in the second-quantized form, then

$$e^{-i\mathbf{q}\cdot\mathbf{r}_2} = e^{-ic\mathbf{P}_K \cdot \mathbf{R}} e^{\frac{-c^2\mathbf{P}_K^2}{4\alpha^2(m_u/c\mu)^2}} e^{\frac{i\mu}{m_2} ic\mathbf{P}_K \cdot \mathbf{a}^\dagger} e^{\frac{i\mu}{m_2} ic\mathbf{P}_K \cdot \mathbf{a}}. \quad (6)$$

Finally, approximately we have

$$\mathcal{L}_\sigma \simeq g_{\sigma K} m_K F(P_k^2) \bar{K} K a_\sigma e^{-ic\mathbf{P}_K \cdot \mathbf{R}}, \quad (7)$$

$$\mathcal{L}_\omega \simeq i g_{\omega K} F(P_k^2) \bar{K} \varepsilon^\mu a_\omega e^{-ic\mathbf{P}_K \cdot \mathbf{R}} \partial_\mu K + \text{H.c.}, \quad (8)$$

with the form factor $F(P_k^2) \equiv \exp[-P_k^2/(4\kappa^2)]$, where $\kappa^2 \equiv \alpha^2(m_u/c\mu)^2$, and $P_k = |\mathbf{P}_K|$.

In the c.m. system of the K -meson, replace $a_\sigma e^{-ic\mathbf{P}_K \cdot \mathbf{R}}$ ($a_\omega \varepsilon^\mu e^{-ic\mathbf{P}_K \cdot \mathbf{R}}$) with σ (ω^μ), Eqs. (7) and (8) can be

*xiaoerqun@yahoo.com.cn

†lilei@nankai.edu.cn

‡zhongxh@ihep.ac.cn

§ningpz@nankai.edu.cn

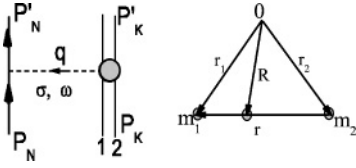


FIG. 1. Feynman diagram for the KN interactions and internal coordinate of two quark system.

rewritten as

$$\mathcal{L}_\sigma \simeq g_{\sigma K} F(P_k^2) m_K \bar{K} K \sigma, \quad (9)$$

$$\mathcal{L}_\omega \simeq i g_{\omega K} F(P_k^2) [\bar{K} \partial_\mu K - K \partial_\mu \bar{K}] \omega^\mu. \quad (10)$$

Comparing with the formulation without considering the quarks coordinates of the K -meson, it is obvious that an additional factor $F(P_k^2)$ appears in the vertexes. Thus, the usual RMF Lagrangian for the KN interaction should be modified as

$$\begin{aligned} \mathcal{L}_K = & \partial_\mu \bar{K} \partial^\mu K - m_K^2 \bar{K} K - g_{\sigma K} m_K F(P_k^2) \bar{K} K \sigma \\ & - i g_{\omega K} F(P_k^2) [\bar{K} \partial_\mu K - K \partial_\mu \bar{K}] \omega^\mu \\ & + [g_{\omega K} F(P_k^2) \omega^\mu]^2 \bar{K} K. \end{aligned} \quad (11)$$

After a few simple deductions [13], we can obtain the real part of the K -nucleus optical potential,

$$\begin{aligned} \text{Re}U = & [g_{\sigma K} m_K \sigma_0 - 2g_{\omega K} E_K \omega_0 - F(P_k^2) (g_{\omega K} \omega_0)^2] \\ & \cdot F(P_k^2) / 2m_K, \end{aligned} \quad (12)$$

which refer to the K -meson three-momenta by the form factor $F(P_k^2)$. The K^- -meson energy E_K can also be deduced from the RMF model [13],

$$E_K = \sqrt{m_K^2 + g_{\sigma K} F(P_k^2) m_K \sigma_0 + P_k^2} - g_{\omega K} F(P_k^2) \omega_0. \quad (13)$$

Here the coupling constants $g_{\sigma K} = 2.088$ and $g_{\omega K} = 3.02$, which are used mostly in the RMF [13].

Up to now the antikaon absorption in the nuclear medium is ignored, since the imaginary potential cannot be obtained

directly from the RMF. Similar to our previous work [13], we assumed a specific form of the imaginary potentials:

$$\text{Im}U = -f \cdot [F_2(P_k^2)]^2 \cdot \left[\frac{E_K}{m_K} W_0 \frac{\rho}{\rho_0} \right], \quad (14)$$

where $F_2(P_k^2) = e^{-P_k^2/(4\beta^2)}$, which is also introduced to modify the imaginary potential (i.e., decay widths) as done in the real part. For the decay width $\Gamma \propto \mathcal{M}^2 \propto g^2$, where \mathcal{M} is the decay amplitude, and g is the coupling, the square of the ‘‘form factor’’ $[F_2(P_k^2)]^2$ is adopted. Besides, the phase space available for the decay products should be considered [14,15], which affects the imaginary potentials (widths). Thus, a factor, f , multiplying imaginary potentials $\text{Im}U$ is introduced in our calculations, as done in Ref. [13] replace $\text{Re}E$ with E_K of Eq. (13)]. The factor f can be assumed to be a mixture of 80% mesonic decay and 20% nonmesonic decay [14,15], thus $f = 0.8f_1 + 0.2f_2$. The imaginary potential parameter W_0 , which is the depth of the imaginary potential at zero momentum, is not determined well. By fitting the K^- -atomic data, $W_0 \sim 50$ MeV [1,2], however, the predictions in Refs. [16,17] give a much deeper value $W_0 \sim 100$ MeV. In this work, we shall discuss several cases for $W_0 = 50, 65, 80$ MeV.

Finally, a momentum-dependent K^- -nuclear potential is obtained. Naturally, we do not expect the naive quark model to give appropriate values for the parameters κ and β . In the calculation, the parameters κ and β are determined by fitting the K -nucleus scattering data. The experimental data of the differential elastic cross sections for K^- - ^{12}C and K^- - ^{40}Ca at $P_k = 800$ MeV/c [6] are used to determine the parameters $\kappa = 0.275$ GeV and $\beta = (0.49, 0.44, 0.42)$ GeV (corresponding to $W_0 = 50, 65, 80$ MeV, respectively). In Fig. 2(a), 2(b), according to the optical potentials from Eqs. (12) and (14), the experimental data are fitted very well. With the determined parameters, we plotted the potentials as functions of kaon three-momentum P_k at normal nuclear density in Fig. 3. The real and imaginary parts are shown in Fig. 3(a) and 3(b), respectively. The solid dotted lines are our calculations

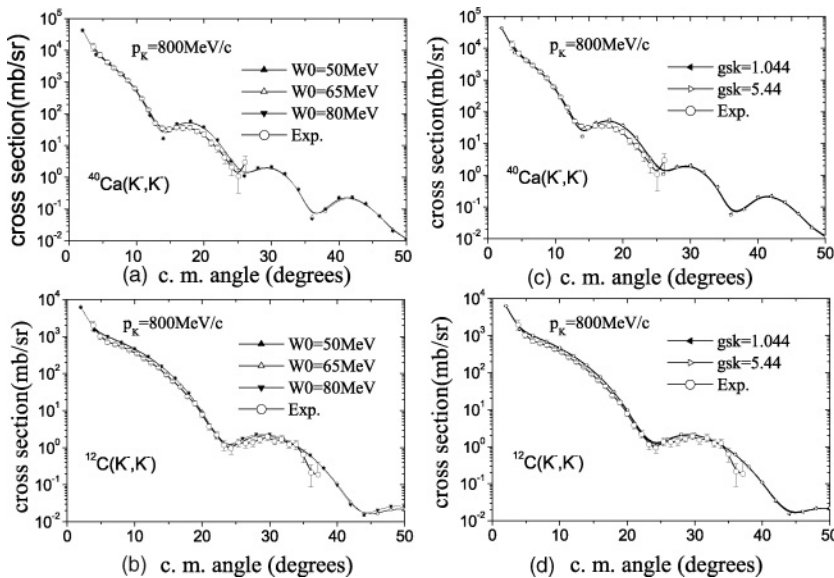


FIG. 2. On several cases of different real (c), (d) and imaginary (a), (b) potentials, the elastic differential cross section for K^- scattering from ^{40}Ca and ^{12}C as functions of the c.m. angles at $p_k = 800$ MeV/c are shown in Figs. (a), (c) and (b), (d), respectively. The experimental data are from Ref. [6].

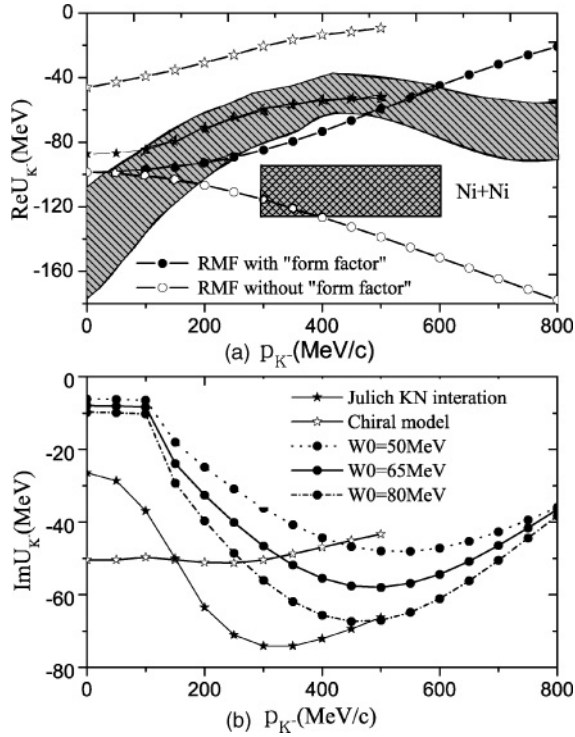


FIG. 3. The real and imaginary antikaon optical potentials in normal nuclear matter based on our model (solid dotted lines) and the other models are shown in (a) and (b), respectively. The solid pentagon's curves are the predictions of a meson-exchange model with the Jülich KN interaction [18]. The hollow pentagon's curves are the results based on the lowest-order meson-baryon chiral Lagrangian (the antikaons and pions are dressed self-consistently) [19]. The shadow region between the two solid curves is the results predicted by Sibirtsev and Cassing (SC model) [4], and the crossed rectangle indicates the results from the analysis of K^- production in Ni+Ni collisions [20,21].

of Eqs. (12) and (14), the potentials predicted by the others [4,18,19] are also presented in the same figure.

From Fig. 3(a), we can see that our results for real potentials decrease with increasing momenta, their varying tendencies are in agreement with the other models [4,18,19]. The depths predicted by us are deeper than those of the chiral and Jülich models. Among these models, the chiral model gives much shallower real potential depths than the other three models. The results of the Jülich KN interaction and RMF model (with form factors) are compatible at $P_K < 600$ MeV, which are almost in the possible region predicted by the SC model. On the other hand, the real potential based on the RMF without “form factor” is also shown in Fig. 3(a). It is obvious that $F_1(P_K^2)$ has a great influence on the real potential, its corrections to the varying tendency of the real potentials are important. From Fig. 3(b), our results of the imaginary potentials increase at first with increasing momenta up to $P_K = 450 \sim 550$ MeV and then decrease, their varying tendencies are similar to the results of Ref. [18]. There is a flat for the imaginary potential curve in the low energy $P_K < 100$ MeV region, which is referred to as the factor $f_1 = 0$, indicating that the total energy ($M_N + E_K$) is less

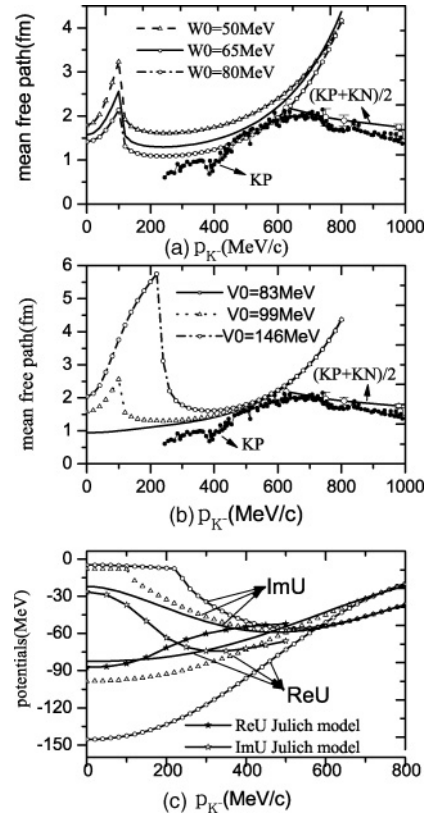


FIG. 4. According to the different imaginary (real) potentials, the K^- mean free paths as functions of the incident momenta in normal nuclear matter are shown in (a) [(b)]. The mean free path from the experimental Kp and $(Kp + Kn)/2$ total cross sections are also presented. Corresponding to the λ_K in (b), the real and imaginary parts of K^- optical potentials are also shown in (c).

than the threshold of $\Sigma\pi$, and the decay channel $NK \rightarrow \Sigma\pi$ is closed.

However, the K^- -nucleus elastic scattering data are not good enough to test the validity of the physics contained in our model. Since little experimental information came directly from the inner nuclei for the kaon, there are many uncertainties in both the real potentials and the imaginary parts. The K^- mean free paths (MFP) in nuclear matter can be calculated with the determined momentum-dependent potentials, which can also be estimated from the experimental data of the total cross sections for K^-p and K^-n [22]. By comparing the results in two different approaches, we expect to find more constraints on the KN interactions.

The details of how to calculate a particle's MFP are given in our previous work [23], only the formula of λ_K is given here:

$$\lambda_K = \frac{1}{2\sqrt{m_K \cdot [B^2 + (\text{Im}U)^2]^{\frac{1}{2}} - m_K \cdot B}}, \quad (15)$$

where, $B \simeq E_K - m_K - \text{Re}U + (E_K - m_K)^2 / 2m_K$. On the other hand, the MFP of K^- is related to the K^-p/K^-n scattering data by a simple relation $\lambda = 1/\rho\bar{\sigma}$, where $\bar{\sigma} = (\sigma_{Kn} + \sigma_{Kp})/2$ is the average of total K^-n and K^-p cross sections. There are some K^-p scattering data in the range of $240 < P_K <$

1000 MeV, and a few data for K^-n scattering in $600 < P_k < 1000$ MeV. Thus only the MFP data from $\bar{\sigma} = (\sigma_{Kn} + \sigma_{Kp})/2$ in the latter region can be compared. The results of two approaches are shown in Fig. 4.

From the figure, we find that $\lambda_p (= 1/\rho\sigma_{Kp})$ is a little larger than $\lambda (= 1/\rho\bar{\sigma})$, and we assume $\lambda_p \approx \lambda$ in the region of $P_k < 600$ MeV. There is a “peak” in each of our calculated curves of the MFP, which is referred to as the factor $f_1 = 0$, corresponding to the position of $M_N + E_K = M_\Sigma + M_\pi$. By comparing the results of different imaginary potential parameter W_0 with the λ_p , and considering $\lambda > \lambda_p$ and $\lambda \approx \lambda_p$, we think the most possible imaginary depth parameter W_0 should be ~ 65 MeV.

If one takes the coupling constant $g_{\sigma K}$ to be a free parameter, the different real potential depths can be obtained by adjusting $g_{\sigma K}$. With $W_0 = 65$ MeV (the corresponding form factor parameter $\beta = 0.44$ GeV), the mean free paths are calculated for the different real potential depths $V_0 = 83, 99, 146$ MeV (the corresponding coupling constant $g_{\sigma K} = 1.044, 2.088, 5.44$), which are shown in Fig. 4(b). The corresponding real and imaginary parts of the optical potentials are also shown in Fig. 4(c). The form factor parameters of the real potential ($\kappa = 0.285, 0.255$ GeV correspond to $g_{\sigma K} = 1.044, 5.44$, respectively) are determined by fitting the K^- nucleus scattering data [which are shown in Fig. 2(c), 2(d)]. From Fig. 4(b), we can see that our calculations of $V_0 = 83$ MeV are most compatible with the λ_p from K^-p scattering data. And in Fig. 4(c), with $V_0 = 83$ MeV and $W_0 = 65$ MeV, both the real and imaginary potentials (the solid curves) of our calculations are very close to those of

the Jülich KN interactions [18] (the star curves) in the range of $P_k < 100$ MeV. It is interesting to see that the recent experiment also indicated that the in-medium K^-N potential depth is about ~ 80 MeV at normal nuclear density [24].

As a whole, with the constraints of the MFP from the KN scattering data, we predicted that the real potential depth is $V_0 \sim 80$ MeV, and the imaginary parameter $W_0 \sim 65$ MeV. One point must be emphasized, if the above results about the potential depths are right, according to our calculations on K^- -nuclei in [13], the sum of the half-widths of the $1s$ and $1p$ states are larger than their separations in K^- -nuclei. In other words, no discrete K^- bound states in the $A \geq 12$ nuclei can be found in experiments.

In conclusion, the momentum dependence of K^- nucleus potentials have been studied in the framework of RMF theory. We think that the interior structure of a kaon may be one of the origin of the momentum dependence, and introduce a “form factor” to correct both the real and imaginary parts of the potential. It is found that the real part of the optical potentials decrease with increasing K^- momenta, however the imaginary potentials increase at first with increasing momenta up to $P_k = 450 \sim 550$ MeV and then decrease. The effects of the exponential form factor on real and imaginary potentials are important.

X.H.Z. would like to thank Prof. H. Oeschler for useful discussions. This work was supported, in part, by the Natural Science Foundation of China (Grand No. 10575054), China Postdoctoral Science Foundation, and the Institute of High Energy Physics, CAS.

-
- [1] E. Friedman, A. Gal, and C. J. Batty, Phys. Lett. **B308**, 6 (1993); Nucl. Phys. **A579**, 518 (1994).
- [2] E. Friedman, A. Gal, J. Mares, and A. Cieplý, Phys. Rev. C **60**, 024314 (1999).
- [3] S. Hirenzaki, Y. Okumura, H. Toki, E. Oset, and A. Ramos, Phys. Rev. C **61**, 055205 (2000).
- [4] A. Sibirtsev and W. Cassing, Nucl. Phys. **A641**, 476 (1998); arXiv:nucl-th/9909024.
- [5] X.-H. Zhong, Lei Li, Chong-Hai Cai, and Ping-Zhi Ning, Commun. Theor. Phys. **41**, No. 4, 573 (2004).
- [6] D. Marlow *et al.*, Phys. Rev. C **25**, 2619 (1982).
- [7] C. Downum *et al.*, Phys. Lett. **B638**, 455 (2006).
- [8] K. Tsushima, K. Saito, A. W. Thomas, and S. V. Wright, Phys. Lett. **B411**, 9 (1997).
- [9] K. Tsushima *et al.*, Phys. Lett. **B429**, 239 (1998); Nucl. Phys. **A630**, 691 (1998).
- [10] Q. Zhao, Phys. Lett. **B636**, 197 (2006); Phys. Rev. D **72**, 074001 (2005); F. E. Close and Q. Zhao, Phys. Rev. D **71**, 094022 (2005).
- [11] N. Isgur, D. Scora, B. Grinstein, and M. B. Wise, Phys. Rev. D **39**, 799 (1989); F. E. Close and A. Wambach, Nucl. Phys. **B412**, 169 (1994).
- [12] R. Kokoski and N. Isgur, Phys. Rev. D **35**, 907 (1987).
- [13] X. H. Zhong, G. X. Peng, L. Li, and P. Z. Ning, Phys. Rev. C **74**, 034321 (2006).
- [14] J. Mares, E. Friedman, and A. Gal, Phys. Lett. **B606**, 295 (2005).
- [15] J. Mares, E. Friedman, and A. Gal, Nucl. Phys. **A770**, 84 (2006).
- [16] N. V. Shevchenko, A. Gal, and J. Mareš, Phys. Rev. Lett. **98**, 082301 (2007).
- [17] V. K. Magas, *et al.*, arXiv:nucl-th/0611098.
- [18] L. Tolos *et al.*, Nucl. Phys. **A690**, 547 (2001).
- [19] A. Ramos and E. Oset, Nucl. Phys. **A671**, 481 (2001).
- [20] W. Cassing and E. L. Bratkovskaya, Phys. Rep. **308**, 65 (1999).
- [21] G. Q. Li, C.-H. Lee, and G. E. Brown, Nucl. Phys. **A625**, 372 (1997).
- [22] W.-M. Yao *et al.*, J. Phys. G **33**, 1 (2006).
- [23] Q. L. Wang *et al.*, Europhys. Lett. **75**, 36 (2006).
- [24] W. Scheinast *et al.*, Phys. Rev. Lett. **96**, 072301 (2006).